Icosahedral Ni Nanowires Formed from Nanocontacts Breaking: Identification and Characterization by Molecular Dynamics

Samuel Peláez[1,*], Pedro A. Serena[1], Carlo Guerrero[2], Ricardo Paredes[3] and Pedro García-Mochales[4]

[1]*Instituto de Ciencia de Materiales de Madrid, Consejo Superior de Investigaciones Científicas, c/Sor Juana Inés de la Cruz 3,Cantoblanco. Madrid - 28049, Spain,* [2]*Centro de Física. Instituto Venezolano de, Investigaciones Científicas. Km. 11 Ctra. Panamericana, Altos de Pipe, Estado Miranda, Venezuela and Departamento de Física, Facultad Experimental de Ciencias, La Universidad del Zulia, Maracaibo, Venezuela,* [3]*Laboratorio de Simulación. Instituto de Matemáticas, Unidad Cuernavaca, Universidad, Nacional Autónoma de México. A. P.273-3 Admon 3. Cuernavaca, Morelos, 62251, México, Departamento de Física y Matemáticas,Universidad Iberoamericana Ciudad de México. Prolongación Paseo de la Reforma 880, Colonia and Centro de Física. Instituto Venezolano de Investigaciones Científicas. Km. 11 Ctra. Panamericana, Altos de Pipe, Estado Miranda, Venezuela. Lomas de Santa Fe, México, D.F. 01219, México,* [4]*Departamento de Física de la Materia Condensada. Facultad de Ciencias, Universidad Autónoma de Madrid. c/Tomás y Valiente 7, Cantoblanco. Madrid - 28049, Spain*

Abstract: We present and discuss an algorithm to identify and characterize the long icosahedral structures (staggered pentagonal nanowires with 1-5-1-5 atomic structure) that appear in Molecular Dynamics simulations of metallic nanowires of different species subjected to stretching. The use of this algorithm allows the identification of pentagonal rings forming the icosahedral structure as well as the determination of its number n_p, and the maximum length of the pentagonal nanowire L_p^m. The algorithm is tested with some ideal structures to show its ability to discriminate between pentagonal rings and other ring structures. We applied the algorithm to Ni nanowires with temperatures ranging between 4K and 865K, stretched along the [111], [100] and [110] directions. We studied statistically the formation of pentagonal nanowires obtaining the distributions of length L_p^m and number of rings n_p as function of the temperature. The L_p^m distribution presents a peaked shape, with peaks located at fixed distances whose separation corresponds to the distance between two consecutive pentagonal rings.

Keywords: Molecular dynamics, metallic nanocontacts, icosahedral nanowires, embedded atom method.

1. INTRODUCTION

Icosahedral (also known as pentagonal) nanowires are formed by subsequent staggered parallel pentagonal rings (with a relative rotation of $\pi/5$) connected with single atoms, showing a characteristic -1-5-1-5- ordering (see an example in Fig. **1a**). The atomic sequence -1-5-1-5- presents a fivefold symmetry with respect to the nanowire axis. This symmetry does not correspond to any crystallographic FCC nor BCC structures. The -1-5-1-5- staggered nanowire configuration may be understood in terms of a sequence of interpenetrated icosahedra. This icosahedral symmetry is quite common in very small systems due to its large stability and high coordination [1]. Metallic nanowires are of great technological importance due to their properties and potential applications as nanoelectronics interconnectors or sensing elements [2,3]. Contrary to monoatomic chains, pentagonal nanowires are rather robust structures at relatively high temperatures and, therefore, they may be considered as a promising candidate for being used as nanodevice components working at realistic conditions. Different computational works during the last decade have shown the formation of staggered pentagonal configurations on breaking nanowires of different species [4-13]. The formation of staggered pentagonal configurations during the stretching process has been already reported for Na [4] using first principles methods, and for Cu [5-8] and Au [9] nanowires with different Molecular Dynamics (MD) approaches. In particular the high stability of the Cu nanowire was confirmed with ab-initio calculations [10]. Pentagonal motives also appear in infinite Al and Pb nanowires obtained from MD simulated annealing methods [11]. More recently such structures have been reported for stretched Ni nanowires with different crystallographic orientations [10,12,13], and confirmed their stability by ab-initio simulations [10,13]. These pentagonal structures are very stable, with lengths larger than 20Å and presenting a high plastic deformation under strain. In general, the reported pentagonal nanowires have been found for simulated single stretching events. However, it is well known that the analysis of nanoscale processes requires the use of statistical approaches since there exist many breaking paths in the nanowire configuration space. Such statistical studies addressing the formation of Ni pentagonal nanowires have been only addressed for Ni up to date [10,12,13]. It has been shown that [100] and [110] stretching directions favor the appearance of long pentagonal nanowires [10-12], and that there exists an optimal temperature at which the pentagonal nanowire yield is maximized [13]. In Refs. [10,12,13] the formation of -1-5-1-5- structures was detected by using a method based on the time Δt_5 that the breaking nanowire lasts with a minimum cross section $S_m \sim 5$ (in units of atoms). The quantity $S_m \sim 5$ is close to the minimum cross-section of a pentagonal ring. As it is shown in Fig. (**1b**), the formation of the pentagonal nanowire (shown in Fig. **1a**) is reflected in the curve of the nanowire minimum cross-section versus time, presenting a long plateau around $S_m \sim 5$ during the pentagonal nanowire formation. A large statistical occurrence of pentagonal nanowires (for a given initial size, orientation and temperature) is reflected in its histogram of minimum cross-section H(S_m) as a huge peak centered at $S_m \sim 5$ (as it is shown in Fig. **1c**). In those previous works, the relative height of that peak or its area has been used to classify the conditions and probability of formation of icosahedral

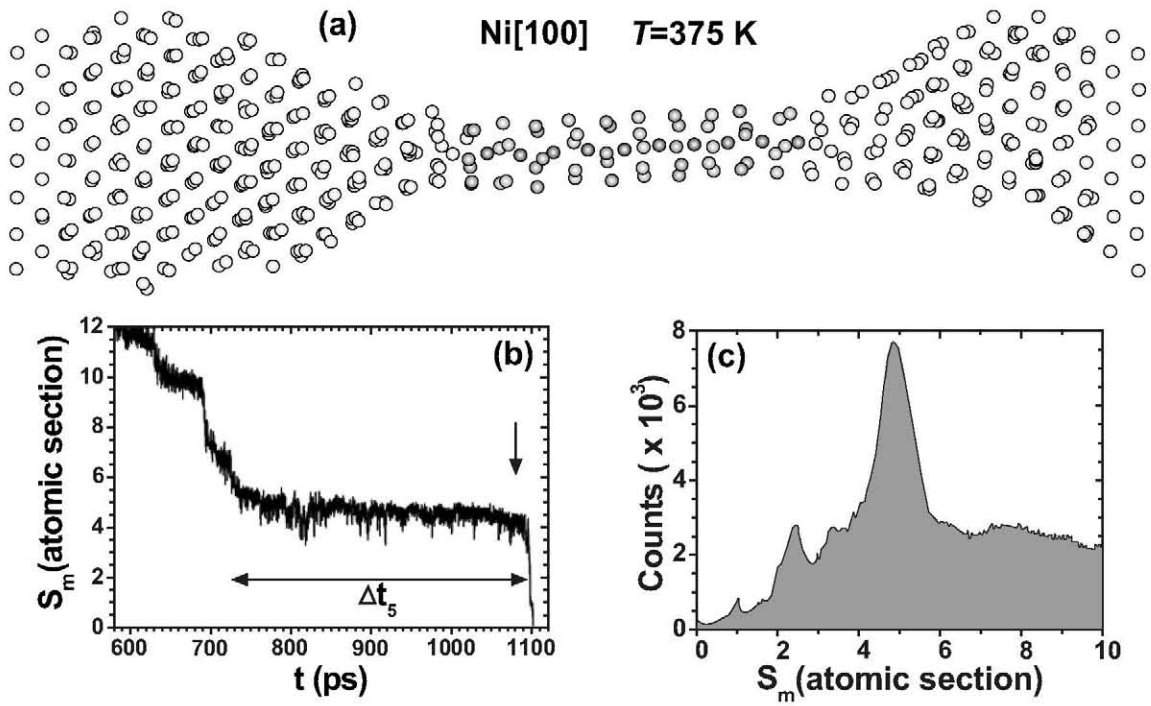

Fig. (1). Results from MD simulations of Ni [100] nanowires containing 1029 atoms and subjected to longitudinal stretching at T = 375K. (**a**) Snapshot of a nanowire formed under stretching presenting an icosahedral structure with n_p = 10 pentagonal rings. (**b**) Minimum cross section $S_m(t)$ curve corresponding to the simulation depicted in (**a**) (the arrow points out the time the snapshot in (**a**) was taken). (**c**) Minimum cross section histogram $H(S_m)$ obtained from the accumulation of 300 independent breaking events.

nanowires, as well as the characterization of individual pentagonal nanowires was made by measuring the duration of plateaus at that cross-section, and associating them a length $\Delta L_5 = \Delta t_5 \times v_S$, where v_S is the stretching velocity. However, this way of measuring ΔL_5 only provides a qualitative value of the average length of the pentagonal nanowires formed under stretching, and gives little information about the actual lengths of such pentagonal chains. Deformations of non-pentagonal regions during the stretching or the existence of stages on the formation of the pentagonal nanowire that provide a cross-section value distant from $S_m = 5$ lead to the miscalculation of the length of the pentagonal region. This method can not determine either the number of pentagonal rings that form the tubular structure. In order to overcome these limitations, in this paper we present an algorithm that allows the automatic identification of pentagonal rings structures as well as the determination of the actual pentagonal nanotube length L_p. With this tool we have revisited the Ni case complementing previous statistical analysis [23] and providing new insight in the formation process leading to pentagonal nanowires.

2. COMPUTATIONAL METHODS

In our study we have followed the same approach of previous papers [14] to perform the simulated nanowire breakage. In short, we have used semi-classical Molecular Dynamics (MD) methods at constant temperature to study the structure and rupture of metallic nanowires. The atomic interactions are described by the Mishin *et al.* parameterization [15] of the embedded atom method (EAM) potentials [16-19]. A nanowire breakage simulation starts with a parallelepiped of atoms ordered according to a FCC structure with bulk Ni lattice parameter a = 3:52Å. The nanowire is stretched along the z coordinate at constant velocity untill the nanowire breaks. During the stretching process the accurate knowledge of the atomic coordinates and velocities allows the characterization of the geometry, forces, and kinetic and potential energies of the stretched nanocontact. The procedure of the breakage simulation and the minimum cross section S_m calculation in atoms units are described in detail in Refs. [10,12,13,18-22].

We are interested in this study on the appearance and identification of icosahedral structures, so we have focused on nanowires stretched along the [111], [100] and [110] directions, in order to compare the probability of observing spontaneous formation of pentagonal nanowires on these different systems. The number of atoms of the simulations is 160, 192 and 204 for the [111], [100] and [110] oriented nanowires respectively. The temperatures used were T =4, 160, 225, 300, 375, 465, 550, 690 and 865 K. This means we are focusing on a range of temperatures below half the bulk Ni melting temperature (T_m =1730K).

In our previous works pentagonal staggered nanowires were tracked by inspecting the minimum cross-section trace in the region $S_m \sim 5$; we defined Δt_5 as the time spent by the nanowire in the $4 < S_m(t) < 6$ region (see Fig. **1b**). This procedure presents two problems. First, it did not allow an exact identification of the simulations creating pentagonal structures. Second, that parameter, when multiplied by the stretching velocity, could not reflect the actual length of the icosahedral nanowire. To overcome these diffculties we have developed an algorithm that identifies the pentagonal rings that form the icosahedral nanowire. The algorithm also allows us to define the pentagonal nanowire length L_p as the distance between the outermost pentagonal rings, and simultaneously, accounting for the number of pentagonal rings n_p that form it.

The algorithm is based in the determination of the angular distribution of the nearest neighbors atoms and provides a position dependent parameter ($\alpha(z)$) which compares the local angular distribution of the projected nanowire atomic coordinates with that corresponding to a perfect pentagonal nanowire. For a given z coordinate we consider a slice perpendicular to the z (stretching) direction with a thickness of 2Å and centered on the z value. The N_t atoms inside such slice are projected onto the xy plane, each one getting new 2D coordinates $\vec{\rho}_i$; then the centroid of this structure is calculated $\vec{\rho}_0 = \sum \vec{\rho}_i / N_t$ The angular distribution is calculated from the angles $\phi_{i,j}$ between the pairs of vectors $\vec{\rho}_i'$ and $\vec{\rho}_j'$ defining the projected atomic coordinates with respect to the centroid ($\vec{\rho}_i' = \vec{\rho}_i - \vec{\rho}_0$). The parameter α is calculated as

$$\alpha = \frac{2}{N_a} \sum_{i,j}^{N_a} \frac{\left|\phi_{i,j} - m\phi_0\right|}{\phi_0},$$

where N_a is the number of pair of atoms considered, $\phi_0 = \pi / 5$ is the reference angle of a perfect staggered pentagonal structure, and m is the integer that minimizes the expression $\left|\phi_{i,j} - m\phi_0\right|$. To avoid spurious contributions from atoms near the pentagonal nanowire axis, only vectors satisfying $\left|\vec{\rho}_i\right| > a/4$ are considered (where a is the distance from the nanowire axis to any atom of the pentagonal ring in the relaxed structure), i.e., those atoms on the chain axis are excluded from the calculation of $\alpha(z)$. This algorithm is applied along the z -coordinate of the nanowire, displacing the imaginary slab δ_z 0.1Å at a time. This results in a function $\alpha(z)$ which will allow us to detect the formation of pentagonal rings as we will explain below.

In order to minimize artifacts, the $\alpha(z)$ curve is averaged over a wider window. This softened curve $\langle\alpha\rangle(z)$ is defined as

$$\langle\alpha\rangle(z) = \frac{1}{\delta_z} \int_{z-\delta_z/2}^{z+\delta_z/2} \alpha(z')dz'$$

where a value of δ_z = 1Å has been found appropriate. This average of $\alpha(z)$ ($\langle\alpha\rangle(z)$) over a 1Å interval provides a quantity that distinguishes between pentagonal and non-pentagonal structures across the nanowire. We have observed that if the parameter $\langle\alpha\rangle(z) < 0{:}5$, the set of atoms around z forms a structure similar to that of a pentagonal ring. In the limit $\langle\alpha\rangle(z) \rightarrow 0$ the nanowire presents an icosahedral symmetry at the z position. On the contrary, if $\langle\alpha\rangle(z) > 0{:}5$ the set of atoms presents another structure (bulk like -FCC, BCC, tetragonal-, helical or disordered). Summarizing, we have developed a function $\langle\alpha\rangle(z)$ with high sensitivity to the presence of pentagonal rings allowing us to distinguish them from other structures with different configurations.

To check the ability of the algorithm to discriminate between different structures in Fig. (**2**) we show the average of $\langle\alpha\rangle$ values obtained using the algorithm along different testing nanowires with increasing amount of disorder. The test structures for the algorithm were: square nanowires with atoms sequence -5-4-5-4- taken from a FCC structure along the [100] direction; staggered pentagonal nanowires with atoms sequence -1-5-1-5-; staggered hexagonal -1-6-1-6- nanowires; and staggered heptagonal nanowires with -1-7-1-7- sequence. The degree of disorder was measured with the mean displacement σ of the atoms from their position in the perfect structure: $\sigma = \sum \left|\vec{\rho}_i - \vec{\rho}_{i,0}\right| / RN_t$ where $\vec{\rho}_{i,0}$ corresponds to the ordered structure atom position, and R is the effective radius of the ordered test configuration. The initial ordered structures (σ = 0) are depicted as inset in Fig. (**2**), and only in the case of pentagonal nanowires the parameter α takes a value 0, being ~1 for the other structures. As the disorder increases, the α average ($\bar{\alpha}$) varies: it increases for pentagonal nanowires and slightly decreases for the other types of nanowires. If the disorder with respect the initial structure is strong enough, the average of α for all the test nanowires converges to a value ~0.9.

In order to further check the ability of the algorithm to identify pentagonal regions, we checked its performance over simulated nanowires showing icosahedral structure. Fig. (**3**) shows a snapshot of a nanowire breaking process where an icosahedral structure is observed. For this snapshot, the $\langle\alpha\rangle(z)$ profile curve is depicted, as well as the radial and angular distribution functions $g(r)$ and $g(\theta)$ through different sections of the nanowire. As illustrated in the figure, the algorithm returns values close to 1 when is applied to the ordered regions of the nanowire, and values well below 1 for the pentagonal region. Minima of $\langle\alpha\rangle$ correspond to the position of the pentagonal rings; as they are not perfect ordered structures (though still can be recognized as pentagons) their $\langle\alpha\rangle$ values are a bit larger than zero. We have arbitrarily chosen the value $\langle\alpha\rangle$ =0.5 as the limit value to recognize a pentagonal structure. As it can be seen in Fig. (**2**), non-pentagonal tubular structures (even with strong disorder) have a $\langle\alpha\rangle$ value higher than 0.5. The pentagonal nanowire, even with a relative strong disorder, presents a $\langle\alpha\rangle$ lower than 0.5; a disordered pentagon with $\langle\alpha\rangle$ > 0.5 can not be identified as a regular one. The value $\langle\alpha\rangle$=0.5 discriminates between pentagonal and non-pentagonal structures. We define the pentagonal nanotube length $L_p(t)$, observed during stretching at a given time t, as the distance between the maximum and minimum z coordinates with $\langle\alpha\rangle$=0.5. This distance corresponds, for long pentagonal chains, to the distance between the two outermost pentagonal rings forming the icosahedral chain. We also define L_p^m as the maximum value of $L_p(t)$ observed when the nanowire is about to break, and n_p is the number of pentagonal rings forming the icosahedral nanowire at its maximum length (equivalent to the number of $\langle\alpha\rangle(z)$ minima below 0.5). The quantities L_p and L_p^m do not include elongation effects coming from the "bulk" regions at the left and right parts of the stretched nanowire.

In Fig. (**3**) we have also divided the nanowire in five regions that seem to have different structures from visual inspection. For each one of these five regions we show the radial and angular distribution functions $g(r)$ and $g(\theta)$. We can see that the outermost regions exhibit a mostly FCC structure, with the FCC typical interatomic distances and angles. The second and fourth sections correspond to an interface which acts as an atomic reservoir that feeds the pentagonal chain. Although it is difficult to identify by visual inspection, the interatomic distances and angles are the same as for the FCC structure. The central region corresponds to the pentagonal structure according to both visual inspection and the $\langle\alpha\rangle(z)$ profile. Inspecting the angular distribution function in this region we can see how the central peak of the FCC structure has disappeared and the peak at the right has displaced a bit towards the left. This is

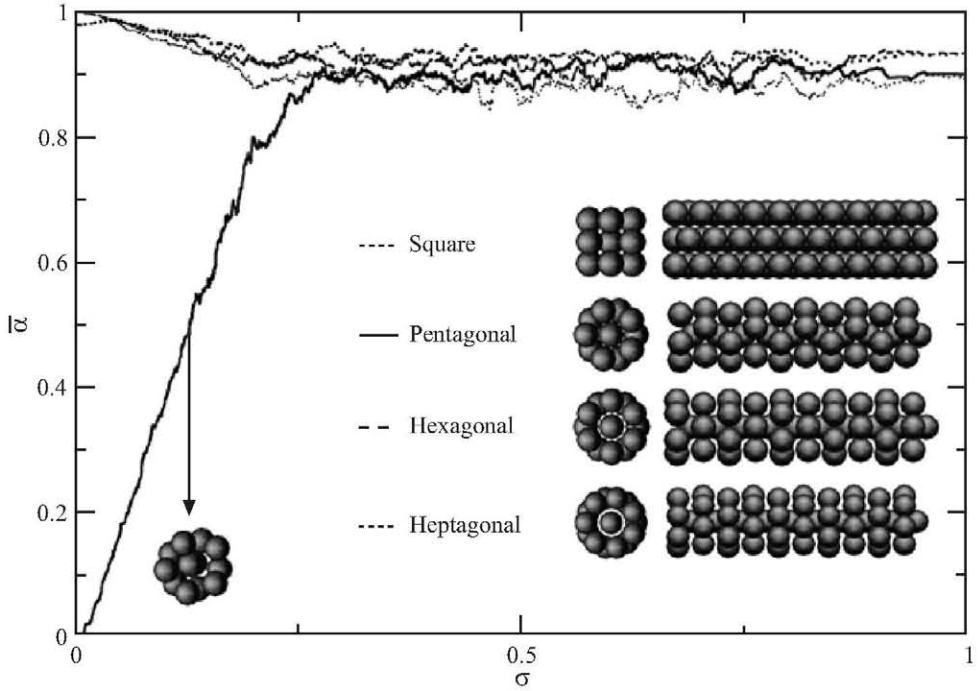

Fig. (2). The average of the α parameter ($\bar{\alpha}$) versus different strengths of the disorder parameter σ (see text) for four test configurations: square -5-4-5-4-, staggered pentagonal -1-5-1-5-, staggered hexagonal -1-6-1-6- and staggered heptagonal -1-7-1-7- nanowires (the inset shows the perfect ordered configurations of the four test nanowires). σ is the mean atomic displacement of atoms with respect to the perfect position of the ordered configuration. The average value of α for disordered nanowires was obtained averaging over 50 configurations.

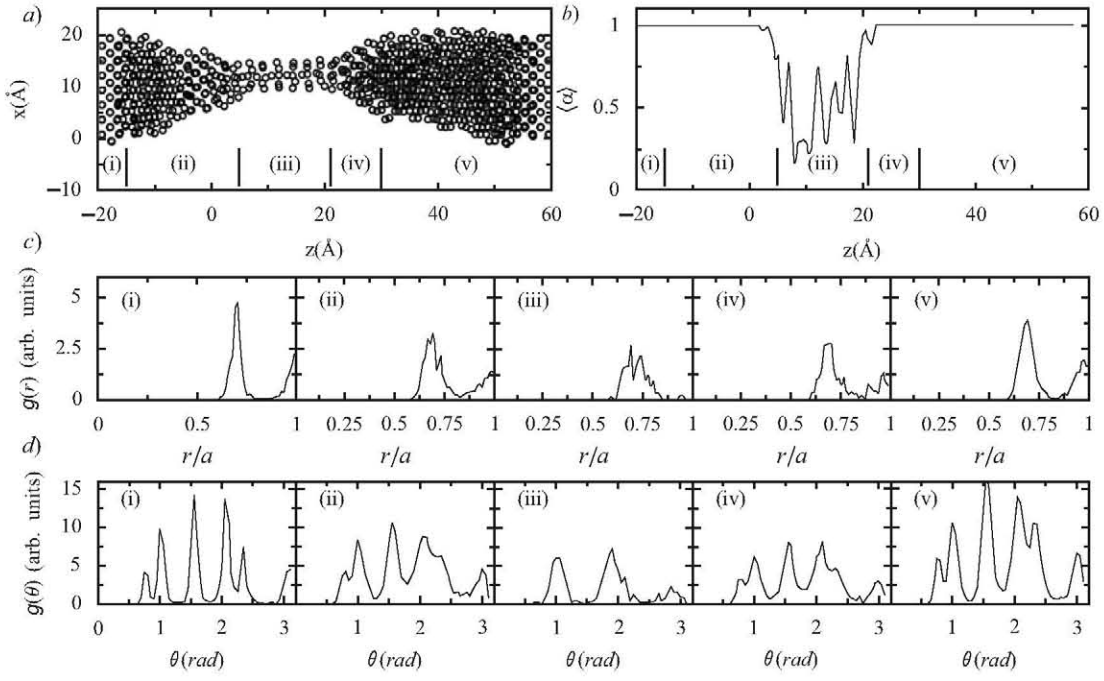

Fig. (3). (**a**) Snapshot of the breaking of a Ni[100] nanowire at T = 375K. (**b**) The $\langle\alpha\rangle$ profile curve is plotted along the z coordinate. For this particular case we also calculated the radial (**c**) and angular (**d**) distribution functions for five different sections of the nanowire. These five sections are defined in (**a**). Notice the change in the angular distribution function of the central (pentagonal) sections, where a central peak around 1.5 has disappeared, a clear characteristic of icosahedral nanowires.

the typical structure of the pentagonal angular distribution function. Regarding the interatomic distances, we cannot appreciate noticeable changes in this region from the radial distribution function. Therefore, $\langle\alpha\rangle$ is a very efficient parameter to identify the pentagonal regions in a breaking nanowire, in comparison to those detection algorithms based on radial distribution functions. It is equivalent to detection algorithms based on angular distributions.

3. RESULTS

Once the ability of the algorithm to identify pentagonal structures has been checked, we apply the algorithm to our simulations

on Ni nanowires. As in previous works the aim is to carry out a statistical study for a broad range of temperatures, obtaining probability distributions of pentagonal nanowires lengths L_p^m and number of pentagonal rings n_p. This will give the optimal temperature required for maximizing their occurrence probability, taking into account that $n_p = 2$ is the minimum value defining a pentagonal nanowire. We compare our results of L_p^m and n_p with the corresponding S_m histograms $H(S_m)$, in order to relate the high peaks in $H(S_m)$ around $S_m \sim 5$ and the presence of pentagonal nanowires. Fig. (**4**) shows the statistics (obtained from 300 simulations for each temperature) of $H(S_m)$, L_p^m and $\boldsymbol{n}_p$ for a set of temperatures ranging from near 0 to $T_m/2$. Only results for [110] oriented nanowires are shown.

In the $H(S_m)$ histograms it is evident the appearance of a peak around $S_m \sim 5$ as the temperature rises. However, beyond T = 550K the height of this peak begins to decrease. This peak reveals the presence of structures that remain at $S_m \sim 5$ for relatively long times. This is the first evidence of the formation of long pentagonal chains during the rupture of the nanowire. For each breaking simulation we have plotted the $\langle\alpha\rangle$ curve and determined the maximum pentagonal length L_p^m and maximum number of pentagonal rings $\boldsymbol{n}_p$. The length L_p^m distributions (Fig. **4b**) present a clearly peaked shape, with the peaks separated approximately by integer values of the distance $d_{5\text{-}5}$ = 2.22Å, the calculated equilibrium separation between successive staggered pentagonal rings [5,8]. The distribution value for $L_p^m = 0$ corresponds to those cases where the nanowire does not form any pentagonal structure ($\boldsymbol{n}_p = 0$). Those cases with $0 < L_p^m <$ 2Å correspond to nanowires showing a unique pentagonal ring ($\boldsymbol{n}_p = 1$). We consider that the nanowire has formed a pentagonal or icosahedral nanowire when $n_p \geq 2$, i.e. when it contains at least a full icosahedron at its narrowest part. The L_p^m distributions from T = 300K to 550K show large tails corresponding to those pentagonal nanowires including a large number of pentagonal rings.

In Fig. (**4c**) the n_p distribution is shown for the same simulations sets. Clearly, for all the temperatures, the most probable case is that the nanowire does not form any pentagonal structure, *i.e.* $n_p = 0$. However for the intermediate range of studied temperatures it is most probable to form a two pentagonal rings structure than that only showing a single ring. Indeed, for two temperatures (375K and 465K) the most probable nanowire structure has 3 staggered pentagons ($n_p = 3$). These two temperatures also exhibit the longest icosahedral structures (see the $n_{p,\max}$ quantities inside the boxes). Ideally every structure with $n_p \geq 2$ would give a sharp peak in the $N(L_p)$ distribution. Since real structures show tilted pentagonal rings, there is not perfect alignment with z-axis and the pentagonal rings separation is longer than that of the equilibrium, producing broad peaks in the $N(L_p)$ figure.

Another interesting analysis in order to determine which conditions favor the appearance of these icosahedral nanowires is based on the calculation of the probability of finding pentagonal chains as a function of the temperature. This is shown in Fig. (**5**) for the three crystallographic orientations that we have simulated. These graphics show that there is an optimal temperature T_{opt} at which the probability of finding pentagonal chains is higher. This optimal temperature, the average value of $\boldsymbol{n}_p$ and the number of planes of its corresponding longest chain are shown in Table **1**.

However the most important observation from Fig. (**5**), is that the probability of getting long pentagonal chains is much lower when breaking along the [111] direction than from the [100] or [110] directions. Fig. (**5**) shows the probability of finding a pentagonal chain with $n_p \geq 2$. For the [111] breaking orientation this probability is below the 20% of the simulations, while for the other orientations, around T_{opt}, the probability is even over 80%. Also in Fig. (**5**) is shown the mean number of pentagonal rings detected in the simulations. Again we see a temperature dependence that gives, at T_{opt}, the longest chains. The shorter pentagonal chains appear when breaking along the [111] orientation. The maximum number of pentagonal rings observed at each temperature $n_{p,\max}$ is also shown. Nanowires broken along the [111] orientation never form chains with more than five pentagonal rings, while this number rises to 14 and 18 for the [100] and [110] orientations respectively.

4. CONCLUSIONS

We have presented a computational method to identify icosahedral nanowires. This methodology also allows the determination of the pentagonal chain length as well as its pentagonal rings. We have tested the proposed algorithm for several ad-hoc ordered and disordered structures, proving that it can satisfactorily distinguish staggered pentagonal nanowires from other tubular structures.

The new methodology has been applied for statistically studying hundreds of Ni breaking nanowire simulations at different temperatures (ranging from 4K to 865K) and along different crystallographic orientations ([111], [100] and [110]), obtaining the pentagonal length L_p^m and number of rings n_p distributions.

The L_p^m distributions show a peaked structure, similar to those found for linear atomic chains [1] with clear peaks separated by integer values of the calculated equilibrium distance between two consecutive staggered pentagons. The $\boldsymbol{n}_p$ distribution shows that the formation of icosahedral structures is not a favorable situation for low and high temperatures. However, there is a range of temperatures (330-730 K) with a large probability (above 70%) of obtaining pentagonal nanowires ($n_p \geq 2$) from stretching processes taking place along the [100] and [100] directions. This temperature dependence of the formation of pentagonal chains opens a technological way to optimize the fabrication of these nanoobjects.

The present results are based on intensive MD simulations and their statistical analysis. This approach to understand the behavior of nanowire mechanical properties requires powerful algorithms to detect specific configurations during the non trivial time evolution from the starting configurations. These identification and characterization algorithms are common to many science branches where in situ analysis is required to detect particular patterns occurring in quasi one-dimensional systems, as it happens in semiconducting nanowires, carbon nanotubes, some surface reconstructions, elongated clusters, DNA chains as well as other biopolymers, etc. In this sense, the concepts underlying the methodology we have developed can be applied to several research fields, taking into account some suitable modifications for improving the capacity of the present method. In relation with the study of the formation of non

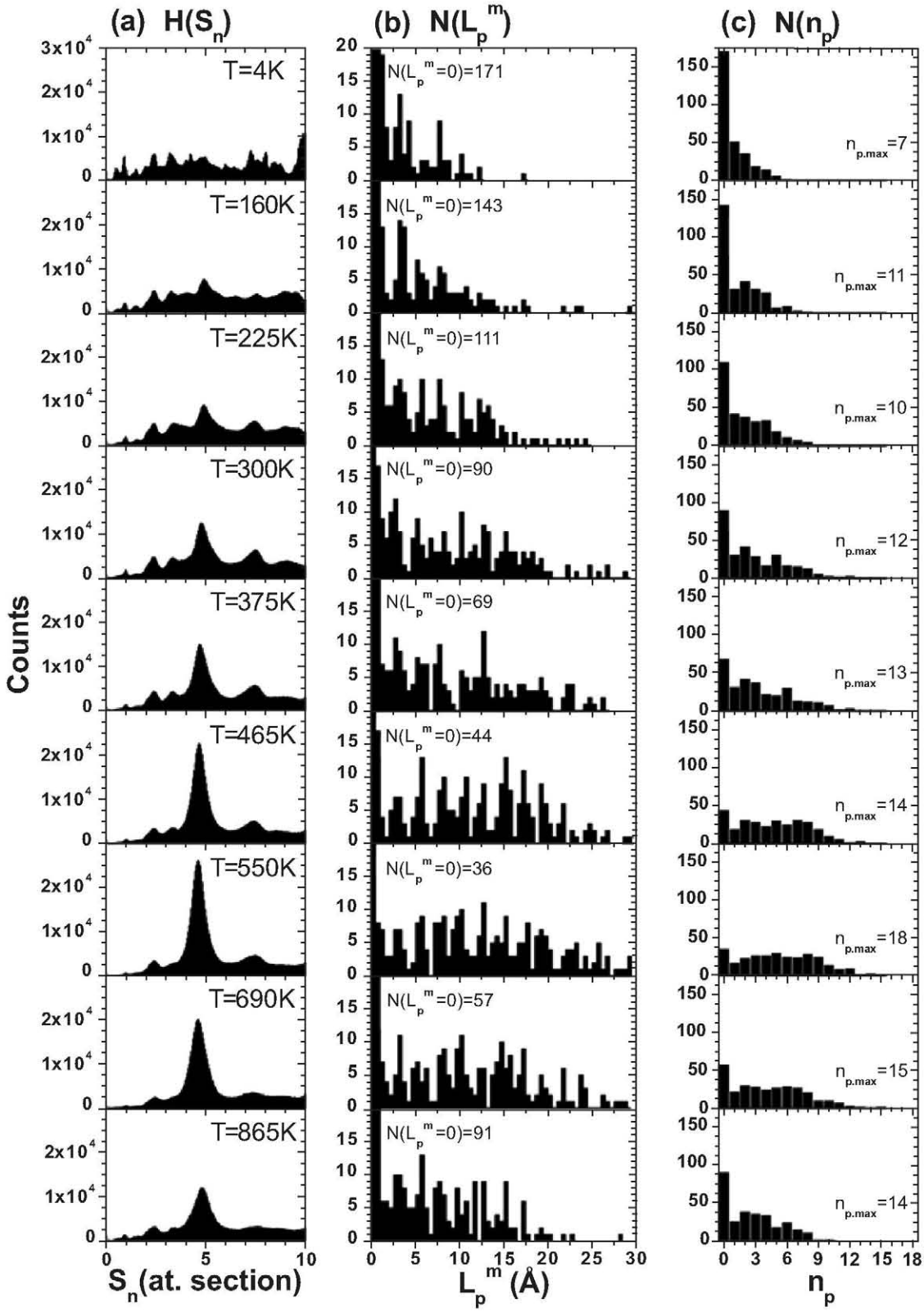

Fig. (4). Distribution function for different quantities obtained from a set of 300 Ni[110] simulated nanowires with a size of 204 atoms. (**a**) Histograms of the nanowire cross sections S_m during the simulation. (**b**) Maximum pentagonal nanowire length L_p^m ; the value $N\left(L_p^m = 0\right)$ corresponds to the number of nanowires from the set of 300 that do not show any pentagonal ring in its structure. (**c**) Number of pentagonal rings n_p just before the pentagonal nanowire breakage (associates with the length L_p^m). Each row corresponds to a different temperature: 4, 160, 225, 300, 375, 465, 550, 690 and 865 K respectively.

Table 1. Optimal Temperature (T_{opt}) at which we have Found the Highest Probability of Finding a Pentagonal Chain ($n_p \geq 2$) and the Maximum Number of Pentagonal Rings Observed at Such T_{opt}

Stretching Direction	[111]	[110]	[100]
T_{opt} (K)	4.65 (0.27 $T_{m,bulk}$)	5.50 (0.32 $T_{m,bulk}$)	5.50 (0.32 $T_{m,bulk}$)
$\langle n_p \rangle$	2.40	5.62	6.39
$n_{p,\max}$	5	14	18

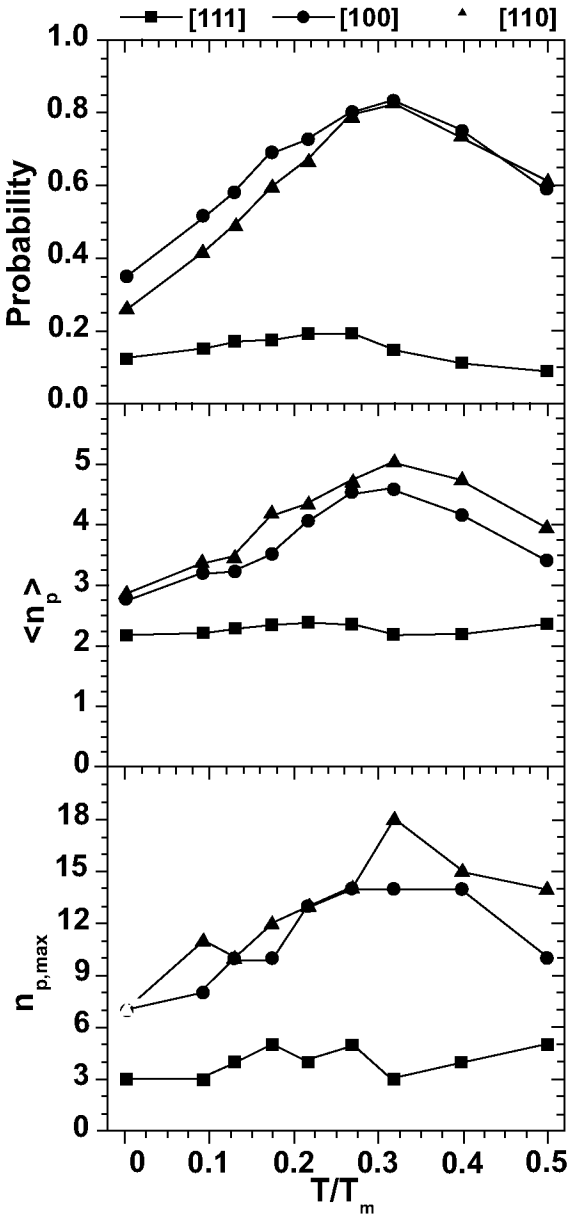

Fig. (5). (**a**) Temperature dependence of the probability of finding pentagonal chains with $n_p \geq 2$. (**b**) Mean number of pentagonal rings. (**c**) Maximum number of such rings detected. This temperature dependence leads to an optimal temperature that favors the formation of long icosahedral chains. Also note that [111] oriented nanowires exhibit the lowest probability of giving long pentagonal chains compared to the other two orientations.

crystalline nanowires the algorithm could include the capacity of detecting new families of nanowires: square, hexagonal, helical and other weird formations. These configurations will be detected from the angular distribution as it has been done for the pentagonal nanowires. Work in such direction is under progress.

ACKNOWLEDGMENTS

This work has been partially supported by the Spanish MICINN through Projects BFM2002- 01167-FISI, FIS2006-1170-C02-01 and CSD2007-00046, and by the Madrid Regional Government through the Programmes S-0505/MAT/0202 (NanoObjetos-CM) and S-0505/TIC/0191 (Microseres-CM). Une of us (PGM also akcnowledges Spanish MEC for the financial support through its "Ramon y Cajal" Programme.

REFERENCES

[1] Bulienkov, N. A.; Tytik, D. L. Modular design of icosahedral metal clusters. *Russian Chem. Bull.*, **2001**, *50*(1), 1-19.

[2] Agraït, N.; Yeyati, A. L.; van Ruitenbeek, J. M. Quantum properties of atomic sized conductors. *Phys. Rep.*, **2003**, *377*, 81-279.

[3] Besenbacher, F.; Olesen, L.; Hansen, K.; Laegsgaard, E.; Stensgaard, I. *Nanowires*. NATO ASI, Ser. E, Kluwer: Dordrecht, **1997**.

[4] Barnett, R. N.; Landman, U. Cluster-derived structures and conductance fluctuations in nanowires. *Nature*, **1997**, *387*, 788.

[5] González, J.; Rodrigues, V.; Bettini, J.; Rego, L.; Rocha, A.; Coura, P.; Dantas, S.; Sato, F.; Galvão, D.; Ugarte, D. Indication of unusual pentagonal structures in atomic-size Cu nanowires. *Phys. Rev. Lett.*, **2004**, *93*(12), 1-4.

[6] Gülseren, O.; Ercolessi, F.; Tosatti, E. Noncrystalline structures of ultrathin unsupported nanowires. *Phys. Rev. Lett.*, **1998**, *80*(17), 3775-3778.

[7] Mehrez, H.; Ciraci, S. Yielding and fracture mechanisms of nanowires. *Phys. Rev. B*, **1997**, *56(19)*, 12632-12642.

[8] Sutrakar, V. K.; Mahapatra, D. R. Formation of stable ultra-thin pentagon Cu nanowires under high strain rate loading. *J. Phys. Condens. Matter.*, **2008**, *20*(33), 335206.

[9] Park, H. S.; Zimmerman, J. A. Stable nanobridge formation in [110] gold nanowires under tensile deformation. *Sci. Mater.*, **2006**, *54*(6), 1127-1132.

[10] García-Mochales, P.; Paredes, R.; Peláez, S.; Serena, P. A. Statistical molecular dynamics study of (111) and (100) Ni nanocontacts: Evidences of pentagonal nanowires. *J. Nanomater.*, **2008**, *2008*, 1-10.

[11] Sen, P.; Gülseren, O.; Yildirim, T.; Batra, I.; Ciraci, S. Pentagonal nanowires: A first-principles study of the atomic and electronic structure. *Phys. Rev. B*, **2002**, *65*(23), 1-7.

[12] García-Mochales, P.; Paredes, R.; Peláez, S.; Serena, P. A. Statistical analysis of the breaking processes of Ni nanowires. *Nanotechnology*, **2008**, *19*(22), 225704.

[13] García-Mochales, P.; Paredes, R.; Peláez, S.; Serena, P. A. The formation of pentagonal Ni nanowires: dependence on the stretching direction and the temperature. *Phys. Status Solidi (a)*, **2008**, *205*(6), 1317-1323.

[14] Díaz, M.; Costa-Krämer, J. L.; Medina, E.; Hasmy, A.; Serena, P. A. Evidence of shell structures in Au nanowires at room temperature. *Nanotechnology*, **2003**, *14*(2), 113-116.

[15] Mishin, Y.; Farkas, D.; Mehl, M.; Papaconstantopoulos, D. Interatomic potentials for monoatomic metals from experimental data and ab initio calculations. *Phys. Rev. B*, **1999**, *59*(5), 3393-3407.

[16] Bratkovsky, A. M.; Sutton, A. P.; Todorov, T. N. Conditions for conductance quantization in realistic models of atomic-scale metallic contacts. *Phys. Rev. B*, **1995**, *52*, 5036.

[17] Daw, M. S.; Baskes, M. I. Semiempirical, quantum mechanical calculation of hydrogen embrittlement in metals. *Phys. Rev. Lett.*, **1983**, *50*, 1285-1288.

[18] García-Mochales, P.; Serena, P. A.; Guerrero, C.; Medina, E.; Hasmy, A. Atomic configurations of breaking nanocontacts of aluminium and nickel. *Mater. Sci.-Poland*, **2005**, *23*(2), 413-419.

[19] Sørensen, M.; Brandbyge, M.; Jacobsen, K. Mechanical deformation of atomicscale metallic contacts: Structure and mechanisms. *Phys. Rev. B*, **1998**, *57*(6), 3283-3294.

[20] García-Mochales, P.; Peláez, S.; Serena, P. A.; Medina, E.; Hasmy, A. Breaking processes in nickel nanocontacts: a statistical description. *Appl. Phys. A*, **2005**, *81*(8), 1545-1549.

[21] Hasmy, A.; Pérez-Jiménez, A.; Palacios, J.; García-Mochales, P.; Costa-Krämer, J. L.; Díaz, M.; Medina, E.; Serena, P. A. Ballistic resistivity in aluminum nanocontacts. *Phys. Rev. B*, **2005**, *72*(24), 2-6.

[22] Rubio-Bollinger, G.; Bahn, S.; Agraït, N.; Jacobsen, K.; Vieira, S. Mechanical properties and formation mechanisms of a wire of single gold atoms. *Phys. Rev. Lett.*, **2001**, *87*(2), 1-4.

[23] Peláez, S.; Guerrero, C.; Paredes, R.; Serena, P. A.; García-Mochales, P.; Identification and characterization of icosahedral metallic nanowires. *Phys. Status Solidi C*, **2005**, *6*(10), 2133-2138.